The Rate of Dissociation Between Antibody and Antigen Determines the Efficiency of Antibody-Mediated Antigen Presentation to T Cells

Pierre Guermonprez,* Patrick England,† Hugues Bedouelle,† and Claude Leclerc[1]*

We analyzed the role of Ab affinity on Ab-mediated Ag uptake and presentation to T cells. Hen egg white lysozyme (HEL) was captured by bifunctional hybrid proteins (Fv-MalE) in which the variable fragment (Fv) of the anti-HEL mAb D1.3 was covalently linked to the *Escherichia coli* MalE protein. These complexes were targeted via two anti-MalE mAbs to an APC expressing a receptor for the Ab constant region. The combination of Fv-MalE and anti-MalE mAbs increased, specifically, HEL presentation. With this experimental system, we evaluated the impact of six different mutations, affecting the Fv-MalE complementarity determining regions, on the increase of HEL presentation by the corresponding hybrids. These mutations increase the dissociation rate constant (k_{off}), and, thus, the dissociation constant of the HEL/Fv-MalE interaction, up to 650-fold, as compared with the wt Fv-MalE. Increasing the k_{off} from 7×10^{-4} s^{-1} up to 300×10^{-4} s^{-1} did not interfere with the enhancement of HEL presentation. A mutant with a k_{off} of 600×10^{-4} s^{-1} had a reduced enhancement ability, and mutants with k_{off} higher than 5700×10^{-4} s^{-1} did not enhance HEL presentation at all. These results show that affinity determines the efficiency of Ab-mediated Ag presentation to T cells. One consequence is that affinity maturation in specific B lymphocytes can drastically enhance their ability to collaborate with T cells in an MHC-restricted way. This may contribute to the selection of high affinity B cell clones. ***The Journal of Immunology,*** **1998, 161: 4542–4548.**

B cells capture and internalize Ags via their specific receptors, the membrane Igs, integrated in the B cell receptor complex (BCR)[2] (1, 2). The interaction of Ag with BCR leads to transmembrane signal transduction and internalization by endocytosis. During endocytosis, peptides generated by the proteolytic degradation of Ag in the endocytic pathway are loaded onto newly synthesized or recycled MHC class II molecules. These complexes are then exported to the cell surface where they are recognized by the TCR of $CD4^+$ T cells (3). In return, B cells receive help from $CD4^+$ T cells for Ab production (4). Besides other factors, the recruitment of T cell help is dependent on the formation of MHC class II/peptide complexes. This formation is greatly dependent on Ag uptake by the APCs. Ab-mediated uptake of Ag by B cells or capture of immune complexes via receptors for the constant region of IgG (FcγR) by other APC has been shown to increase greatly Ag presentation to T cells (3, 5).

In the course of the T cell-dependent humoral response to many haptens, the detailed analysis of Ab affinity (at the serum level, or at the clonal level) revealed a decrease in the dissociation constant (K_d) from $10^{-5}/10^{-6}$ M in the primary response to $10^{-7}/10^{-8}$ M in the late response after booster injections (6). This progressive increase of affinity has not been observed for other T cell-dependent Ag such as monomeric hen egg white lysozyme (HEL). In these cases, the Ab affinity reaches a high level ($K_d = 10^{-7}/10^{-10}$ M) a few days after a primary injection and does not increase after booster injections (7).

In the present study, we analyzed the role of the affinity of Ab for Ag on the efficiency of Ab-mediated Ag presentation to $CD4^+$ T cells. We chose to address this question with HEL, which is a monomeric protein Ag. We have previously demonstrated in vitro the enhancing effect of the anti-HEL mAb D1.3 on the presentation of HEL to a specific T cell hybridoma (anti-HEL 108–116, I-E^d) by an FcγR-expressing APC (P.Guermonprez et al., manuscript in preparation). In the present study, HEL was captured by a bifunctional hybrid protein (Fv-MalE) (8) formed between the variable fragment (Fv) of the anti-HEL mAb D1.3 and the *Escherichia coli* maltose-binding protein (MalE) in the presence of two anti-MalE mAbs. Different Fv-MalE hybrids were prepared with mutations in the D1.3 complementarity determining regions (CDR), leading to reduced affinities for HEL (9). Thus, in this experimental model, the internalization of Fv-MalE hybrids is therefore fixed to a stable level that is independent of the HEL concentration. Affinity variations between Fv-MalE and HEL were determined with precision, opening the possibility of a quantitative analysis of the role of affinity on Ab-mediated Ag presentation. The effects of these hybrids on HEL presentation to a specific T cell hybridoma were then compared with those obtained with the wt D1.3 Fv-MalE. The results of this study show that an increase of HEL presentation to T cells occurred through the interaction of the Fc regions of the anti-MalE mAbs with the FcγR of the APC. This experimental system allowed us to show that the affinity of anti-HEL Abs determines the efficiency of Ab-mediated Ag presentation to T cells.

*Unité de Biologie des Régulations Immunitaires and †Groupe d'ingénierie des protéines (Centre National de la Recherche Scientifique URA1129), Unité de Biochimie Cellulaire, Institut Pasteur, Paris, France

Received for publication March 17, 1998. Accepted for publication June 24, 1998.

The costs of publication of this article were defrayed in part by the payment of page charges. This article must therefore be hereby marked *advertisement* in accordance with 18 U.S.C. Section 1734 solely to indicate this fact.

[1] Address correspondence and reprint requests to Dr. Claude Leclerc, Institut Pasteur, 25 rue du Docteur Roux 75724 Paris, Cedex 15, France. E-mail address: cleclerc@pasteur.fr

[2] Abbreviations used in this paper: BCR, B cell receptor complex; FcγRIIb2, b2 isoform of the type II receptor for the constant region of IgG; HEL, hen egg white lysozyme; MalE, maltose-binding protein of *Escherichia coli*; Fv-MalE, hybrid formed between the MalE protein and the variable regions of the anti-HEL D1.3 mAb; K_d, dissociation constant; K'_d, dissociation constant calculated with the BIAcore apparatus; k_{off}, rate of dissociation; k_{on}, rate of association; V_H, V region heavy chain; V_L, V region light chain; CDR, complementarity determining region; wt, wild-type; EF, enhancement factor.

0022-1767/98/$02.00

Materials and Methods

Ags and mAbs

HEL was purchased from Sigma (St. Louis, MO). Peptide 108–116 from the HEL sequence (p108–116, WVAWRNRCK) was synthetized by Neosystem (Strasbourg, France). The D1.3 anti-HEL B cell hybridoma (IgG1, κ) was a kind gift from Dr. Poljak (Center for Advanced Research in Biotechnology, Rockville, MD) (10). The mAb D1.3 was obtained from ascitic fluid from BALB/c mice and precipitated with ammonium sulfate, then resuspended in purified water and extensively dialyzed against PBS. Protein concentration was determined with a colorimetric assay (Bio-Rad, Münich, Germany). The anti-MalE mAbs 94.1 and 56.5 (IgG1, κ) were a kind gift of Dr. J. C. Mazié (Institut Pasteur, Paris, France).

Fv-MalE hybrids and their mutants

Fully functional variable fragments (Fv) of D1.3, a mouse mAb directed against HEL (10), were produced as hybrids (Fv-MalE) with the maltose-binding protein of *E. coli* (MalE). The production and purification of the Fv-MalE hybrids and their mutants has been previously described (8, 9). In the case of V_L::V_H-MalE hybrids, the variable region of the H chain (V_H) is genetically coupled to the N terminus of MalE and noncovalently associated with the variable domain of the L chain (V_L). In the opposite case (V_H::V_L-MalE), the variable region of the L chain (V_L) is genetically coupled to the N terminus of MalE and noncovalently associated with the variable domain of the H chain (V_H). For both constructs, site-directed mutations have been constructed in the complementarity determining regions (CDR) of the H or L chain of D1.3. The kinetics of interaction between HEL and the wt or mutant hybrids have already been described (9). The characteristics of the different Fv-MalE hybrids used in this study are summarized in Table I.

Analysis of the binding between the anti-MalE mAbs and Fv-MalE/HEL complexes with the BIAcore technology

HEL was covalently immobilized on the carboxymethylated dextran surface of a CM5 sensorchip to a level of 2700 resonance units (RU), using the Amine Coupling Kit (Pharmacia Biosensor, Uppsala, Sweden). The resulting derivatized surface, CM5-HEL, was equilibrated with buffer M at a temperature of 20°C and a flow rate of 5 μl/min, conditions that were used in all subsequent steps. Buffer M was 10 mM phosphate buffer (pH 7.4), 2.7 mM KCl, 137 mM NaCl, 0.005% detergent P20 (Pharmacia), and 1 mM maltose. The addition of maltose prevents any dimerization of MalE (9). For all binding experiments, samples were diluted in buffer M.

Cell lines

A20 (A^d/E^d), a B cell lymphoma line originated from BALB/c mice (11), and IIA1.6, an FcγR-deficient variant of A20 (12), have been described. A6B9, a stable transfectant of IIA1.6 for the b2 isoform of the murine type II weak affinity receptor for IgG (FcγRIIb2) (13), was used as APC and was kindly provided by C. Bonnerot and S. Amigorena (Institut Curie, Paris, France). The L3E10 T cell hybridoma, which is specific for the HEL 108–116 T cell epitope (WVAWRNRCK), I-E^d restricted, was produced using BALB/c mice immunized with HEL (14). The CTLL cell line was purchased from the American Type Culture Collection (ATCC, Manassas, VA).

Ag presentation assay

HEL and/or anti-HEL Fv-MalE and/or a mixture of the two anti-MalE mAbs 94.1 and 56.5 were mixed together for 1 h at 37°C, in a final volume of 0.1 ml of complete medium (RPMI 1640 medium supplemented with 10% FCS, 100 U/ml penicillin, 100 μg/ml streptomycin, 2 mM L-glutamine, and 5×10^{-5} M 2-ME) in 96-well flat-bottom culture microplates. The concentrations used in each experiment are indicated in the figure legends. Then, L3E10 T cell hybridoma cells (10^5 cells/well) were cocultured with A6B9 (10^5 cells/well) and the preformed complexes (HEL, anti-HEL Fv-MalE, and anti-MalE mAbs) for 24 h in 0.2 ml (final volume) of complete medium. After 24 h, the supernatants were frozen for at least 2 h at −70°C. Then, 10^4 cells/well of the CTLL cell line, which proliferates specifically in response to IL-2 but not IL-4, were cultured with 100 μl of supernatant in 0.2 ml final volume. Two days later, [^{3}H]thymidine (NEN Life Science, Boston, MA) was added, and the cells were harvested 18 h later with an automated cell harvester (Skatron, Lier, Norway). Incorporated thymidine was detected by scintillation counting. To block FcγR, the A6B9 APC were incubated 30 min at 4°C with the anti-FcγRII/III mAb 2.4G2 (15) (PharMingen, San Diego, CA) at 10 μg/ml, then washed before use for Ag presentation assay. In all experiments, each point was done at least in duplicate and more often in triplicate.

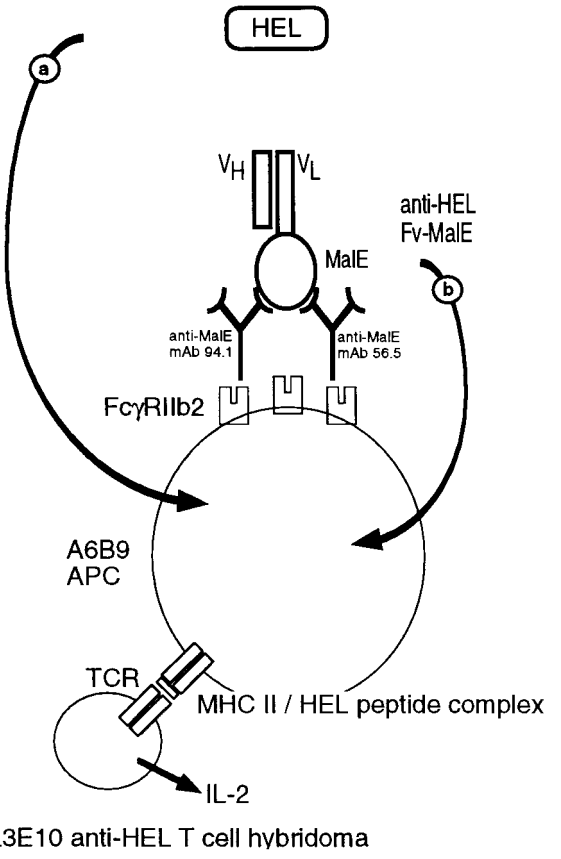

FIGURE 1. Experimental system used in this study. HEL is presented to the L3E10-specific T cell hybridoma (anti-HEL108-116, I-E^d) by the A6B9 B cell lymphoma (H-2^d, FcγRIIb2^+) APC. HEL is captured by nonspecific pinocytosis in fluid phase (a) or by FcγRIIb2-mediated endocytosis in presence of anti-HEL Fv-MalE hybrids and the two anti-MalE mAbs 94.1 and 56.5 (b). More details are given in *Materials and Methods*.

Results

Anti-HEL Fv-MalE enhances HEL presentation to a T cell hybridoma in the presence of anti-MalE mAbs

In a previous study, we analyzed the effect of the anti-HEL mAb D1.3 and other anti-HEL mAbs on the presentation of HEL to the specific T cell hybridoma L3E10 (anti-HEL 108–116, I-E^d restricted) by the A6B9 APC (A^d/E^d), which is a B cell lymphoma transfected with the b2 isoform of the type II murine FcγR (FcγRIIb2). FcγRIIb2 is implicated in Ag presentation, unlike FcγRIIb1, and is physiologically expressed by professional APC (13). We have shown that the anti-HEL mAb D1.3 increases significantly the efficiency of HEL presentation. This effect is HEL specific, T cell epitope specific, independent of a nonspecific activation of the APC, and dependent on FcγRIIb2-mediated uptake (P.Guermonprez et al., manuscript in preparation). In the present report, we analyzed the effect of the anti-HEL D1.3 Fv-MalE on the presentation of HEL to the same T cells by the same APC, in the presence of two anti-MalE mAbs (Fig. 1). Fv-MalE hybrids are formed by genetically fusing the Fv of the anti-HEL mAb D1.3 with the MalE protein.

To assess the effect of the anti-HEL Fv-MalE on the presentation of HEL, we stimulated an HEL-specific T cell hybridoma in the presence of the A6B9 APC. The HEL-specific T cell hybridoma used in this study, L3E10, recognizes the immunodominant HEL epitope 108–116 complexed with I-E^d. The titration experiment shown in Figure 2*A* revealed that the concentration of HEL

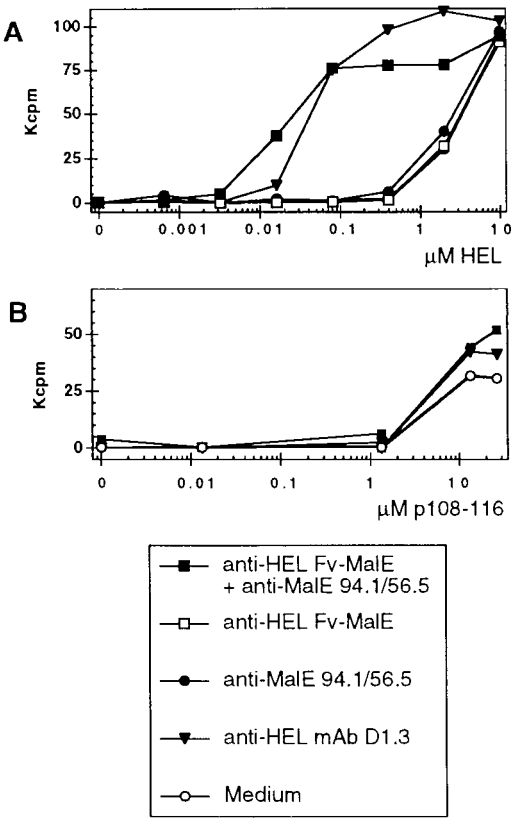

FIGURE 2. Anti-HEL Fv-MalE enhances specifically the presentation of HEL to a specific T cell hybridoma in the presence of anti-MalE mAbs. The L3E10 T cell hybridoma (anti-HEL108-116, I-E^d) was cocultured with the A6B9 B cell lymphoma (H-2^d, FcγRIIb2^+) in the presence or absence of various concentrations of Ag (*A*, HEL; *B*, synthetic peptide p108–116) for 24 h. The cultures were done 1) with medium alone, 2) in the presence of the anti-HEL mAb D1.3 (at 0.167 μM), 3) in the presence of an anti-HEL Fv-MalE hybrid (V_H::V_L-MalE (wt)), corresponding to the variable regions of the mAb D1.3, used at 0.167 μM and/or of a mixture of two anti-MalE mAbs, 94.1 and 56.5 (0.03 μM each). The complexes were formed before addition to the cultures of A6B9 and L3E10, as described in *Materials and Methods*. The IL-2 released by L3E10 after 24 h of culture with A6B9 was assessed by the CTLL proliferation assay. Results are expressed in kcpm.

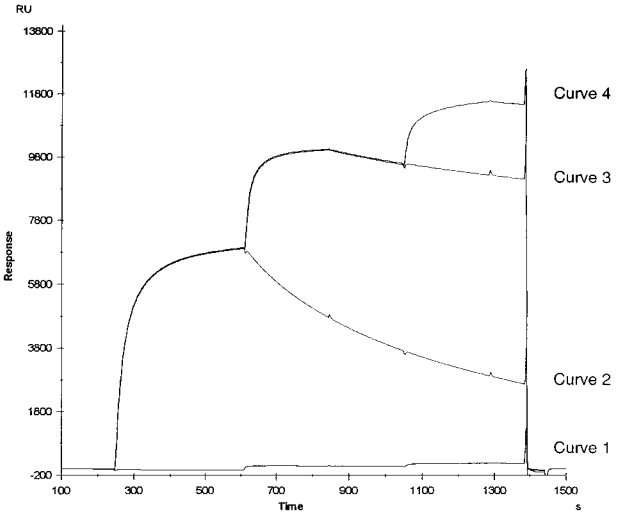

FIGURE 3. Binding assay performed with the BIAcore apparatus for the detection of tetramolecular complexes between HEL, anti-HEL V_H::V_L-MalE, anti-MalE mAb 94.1, and anti-MalE mAb 56.5. HEL was immobilized on a sensorchip as described in *Materials and Methods*. Each curve shown here represents the signal obtained on the HEL surface after subtraction of the background signal obtained on a mock derivatized control surface. After each injection, the surface was regenerated by injection of 5 μl of 50 mM HCl. All curves represent a sequence of six different serial injections performed at 5 μl/min at 243 s, 609 s, 842 s, 1051 s, 1289 s, and 1382 s. The different curves represent different experiments with the following sequence for the six injections: curve 1, buffer M/anti-MalE mAb 94.1/buffer M/anti-MalE mAb 56.5/buffer M/50 mM HCl; curve 2, anti-HEL V_H::V_L-MalE/buffer M/buffer M/buffer M/buffer M/50 mM HCl; curve 3, anti-HEL V_H::V_L-MalE/anti-MalE mAb 94.1/buffer M/buffer M/buffer M/50 mM HCl; curve 4, anti-HEL V_H::V_L-MalE/anti-MalE mAb 94.1/buffer M/anti-MalE mAb 56.5/buffer M/50 mM HCl. Protein samples injected were diluted in buffer M and the concentrations were 25 μg/ml for V_H::V_L-MalE and 50 μg/ml for the anti-MalE mAbs.

required to obtain a half optimal T cell stimulation (assessed by IL-2 release) was about 50-fold less in the presence of the anti-HEL mAb D1.3 than in its absence. A similar enhancement of HEL presentation was obtained with a mixture of an anti-HEL Fv-MalE, derived from mAb D1.3, and of the two anti-MalE mAbs 94.1 and 56.5. Anti-HEL Fv-MalE alone or the mixture of the anti-MalE mAbs 94.1 and 56.5 alone was without effect on the presentation of HEL to the L3E10 T cell hybridoma. The mixture of anti-HEL Fv-MalE plus the two anti-MalE mAbs 94.1 and 56.5, or the anti-HEL mAb D1.3 alone, were without effect on the presentation of the synthetic HEL peptide 108–116 to the specific T cell hybridoma L3E10 (Fig. 2*B*). These results demonstrated that the enhancement effect observed with Fv-MalE in the presence of anti-MalE mAbs was specific of HEL presentation and involved the antigenic recognition of HEL by the Fv-MalE molecule.

Tetramolecular complexes are formed between HEL, anti-HEL Fv-MalE, and anti-MalE mAbs 94.1 and 56.5

The lack of effect of anti-HEL Fv-MalE on HEL presentation in the absence of anti-MalE mAbs suggested that the complexes formed between anti-HEL Fv-MalE and HEL were recognized by the anti-MalE mAbs. The reactivity of the anti-MalE mAb 56.5 toward the MalE component of anti-HEL Fv-MalE has already been described (9). We further analyzed the ability of the two different anti-MalE mAbs to bind the complex formed between anti-HEL Fv-MalE and HEL by using the BIAcore technology (Fig. 3). The simultaneous recording of signals obtained in each experiment, both on a control surface (mock-derivatized) and on a surface derivatized with HEL, allowed us to subtract the signal, due only to changes in the refraction index of the buffers and/or to the nonspecific binding of compounds on the dextran matrix of the sensorchip, from the specific signal obtained on the HEL surface. The comparison of curves 1 and 2 demonstrated that Fv-MalE specifically associated with HEL. The comparison of curves 2 and 3 showed the specific association of the anti-MalE mAb 94.1 to the HEL/Fv-MalE complex. The comparison of curves 3 and 4 showed the specific binding of the anti-MalE mAb 56.5 to the HEL/Fv-MalE/94.1 complex. Similar results were obtained when inverting the order of binding of the two anti-MalE mAbs (data not shown). These results therefore showed that both anti-MalE mAbs could bind simultaneously to the HEL/anti-HEL Fv-MalE complex.

The enhancement of HEL presentation by anti-HEL Fv-MalE in the presence of anti-MalE mAbs is FcγRIIb2 mediated

We reported above that the enhancement of HEL presentation by Fv-MalE depended on the anti-MalE mAbs. In particular, the stimulation of L3E10 by A6B9 at a suboptimal concentration of HEL

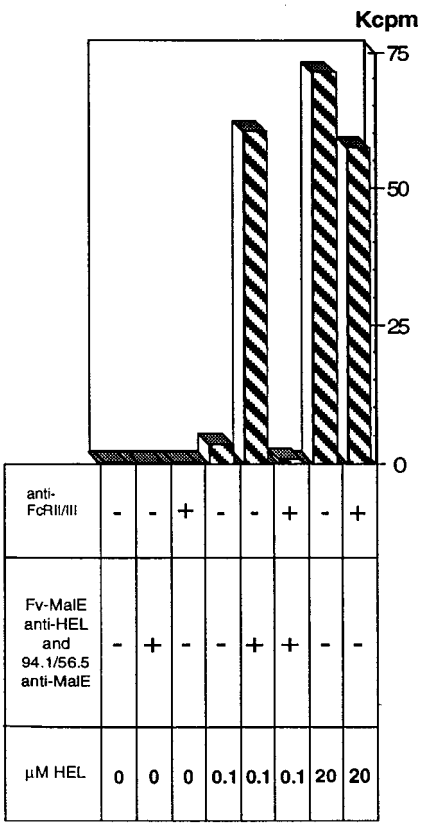

FIGURE 4. Enhanced presentation of HEL in the presence of the anti-HEL Fv-MalE and of the anti-MalE mAbs 94.1 and 56.5 is FcγRIIb2 dependent. The L3E10 T cell hybridoma (anti-HEL108-116, I-E^d) was co-incubated for 24 h with the A6B9 B cell lymphoma (H-2^d, FcγRIIb2$^+$) in the presence or absence of various concentrations of HEL (0.1 or 20 μM), of anti-HEL Fv-MalE (V_H::V_L-MalE (wt), at 0.2 μM) plus a mixture of two anti-MalE mAbs, 94.1 and 56.5 (0.13 μM each). In some experiments, the A6B9 APC was preincubated 30 min at 4°C with the anti-FcγRII/III mAb 2.4G2 (10 μg/ml) and then washed before the incubation with L3E10 and HEL. The IL-2 released by L3E10 after 24 h of coculture with A6B9 was assessed by the CTLL proliferation assay. Results are expressed in kcpm.

(0.1 μM) was fully dependent on the presence of the Fv-MalE/anti-MalE mAb complex (see Fig. 2*A*). This dependence suggested that the complex formed between Fv-MalE and HEL was efficiently captured by the APC via the FcγRIIb2 receptor. To test this hypothesis, we blocked FcγRIIb2 by preincubating the A6B9 APC with the anti-FcγRII/III mAb 2.4G2. This mAb has been shown to inhibit the Fc/FcγR interaction (15). The L3E10 response to the mixture of 0.1 μM HEL, Fv-MalE, and anti-MalE mAbs was completely abolished by the preincubation of the A6B9 APC with mAb 2.4G2 (Fig. 4). In a previous study, we showed that this mAb also totally and specifically blocked the D1.3-mediated increase of HEL presentation by A6B9 (P. Guermonprez et al., manuscript in preparation). In contrast, the preincubation treatment of A6B9 with mAb 2.4G2 did not interfere with the stimulation of L3E10 at an optimal concentration of free HEL (20 μM). These results showed that formation of complexes between HEL, anti-HEL Fv-MalE, and the two anti-MalE mAbs 94.1 and 56.5 resulted in the efficient uptake of HEL via the FcγR of APC, which, in turn, led to a more efficient presentation of HEL to the L3E10 T cell hybridoma.

The enhancement of HEL presentation depends on the affinity of Fv-MalE for HEL

To quantitatively measure the contribution of the affinity between Fv-MalE and HEL to the enhancement of HEL presentation, we used mutants of the anti-HEL Fv-MalE. The mutations affected residues of the light or heavy chain CDRs (Table I). All the mutant Fv-MalE are derived from the anti-HEL mAb D1.3, they had the same specificity, and their reduced affinity for HEL was mainly due to an increase of their dissociation rate constant (k_{off}) (9). We measured the stimulation of the L3E10 T cell hybridoma in the presence of HEL at various concentrations, of each mutant anti-HEL Fv-MalE at a fixed concentration (0.2 μM), and of the anti-MalE mAbs 94.1 and 56.5 also at fixed concentrations (0.13 μM each). A representative experiment is shown in Figure 5*A*. The two wt hybrids, which have virtually the same affinity for HEL, gave an identical enhancement of HEL presentation. These hybrids have the Fv of the anti-HEL mAb D1.3 in different configurations, V_H::V_L-MalE (wt) or V_L::V_H-MalE (wt). Thus, the fusion of either the V_H or the V_L region to the N terminus of MalE does not interfere with the enhancement of HEL presentation by the anti-HEL Fv-MalE hybrids. We then examined the effects of six different mutations in V_L (Y50F or Y32F or W92A) or in V_H (Y101F or D100N or D54A). The enhancement of HEL presentation observed in the presence of V_H::V_L-MalE(Y50F) or V_H::V_L-MalE(Y32F) or V_L::V_H-MalE(D54A) was similar to that induced by V_H::V_L-MalE (wt) or V_L::V_H-MalE (wt) (Fig. 5*A* and data not shown for V_L::V_H-MalE(D54A)). The enhancement was significantly lower for V_L::V_H-MalE(Y101F) than for the wt hybrids. V_L::V_H-MalE(D100N) and V_H::V_L-MalE(W92A) virtually did not enhance the HEL presentation (Fig. 5*A* and data not shown for V_H::V_L-MalE(W92A)). In these experiments, the internalization of the different Fv-MalE mutants by the APC did not vary since it depended on the complexation of the Fv-MalE with the

Table I. *Anti-HEL Fv-MalE hybrids*

Type of Construct[a]	Mutation	Mutation Location	k_{on} (10^4 $M^{-1} \cdot s^{-1}$)	k_{off} (10^{-4} s^{-1})	$t_{1/2}$[b] (s)	K'_d[c] (nM)
V_L::V_H-MalE	wt	none	7.84 ± 0.45	6.66 ± 0.79	1,036	8.46 ± 0.73
V_H::V_L-MalE	wt	none	8.66 ± 1.02	7.51 ± 0.29	919	8.96 ± 0.91
V_H::V_L-MalE	Y50F	L-CDR2	8.76 ± 0.37	17.7 ± 0.5	390	20.3 ± 0.3
V_L::V_H-MalE	D54A	H-CDR2	11.8 ± 0.7	186 ± 12	37	163 ± 22
V_H::V_L-MalE	Y32F	L-CDR1	8.24 ± 0.16	294 ± 6	23	357 ± 12
V_L::V_H-MalE	Y101F	H-CDR3	9.68 ± 0.31	622 ± 27	11	643 ± 43
V_L::V_H-MalE	D100N	H-CDR3	20.7 ± 3.6	10,300 ± 1,000	0.7	5,000 ± 400
V_H::V_L-MalE	W92A	L-CDR3	11.1 ± 0.6	5,700 ± 400	1.2	5,120 ± 590

[a] In the V_L::V_H-MalE (V_H::V_L-MalE) hybrid, V_H (V_L) is covalently linked to MalE and non covalently associated with V_L (V_H).
[b] $t_{1/2}$, The half life of complexes between hybrids and HEL. $t_{1/2} = Ln(2)/k_{off}$
[c] K'_d, The equilibrium dissociation constant between Fv-MalE and HEL measured at 20°C with the BIAcore apparatus at the heterogeneous interface between the liquid phase and the sensorchip.

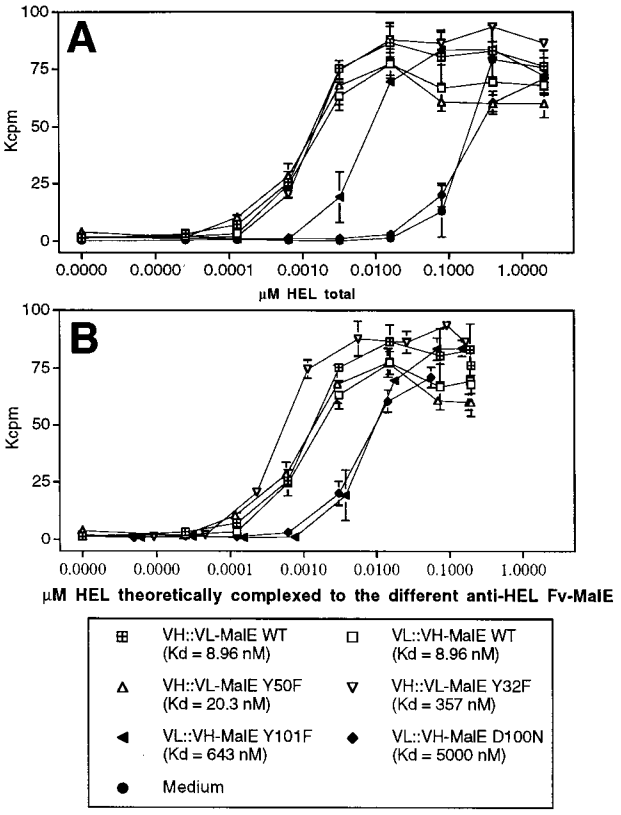

FIGURE 5. The enhancement of HEL presentation by anti-HEL Fv-MalE in the presence of anti-MalE mAbs is dependent on the affinity of Fv-MalE for HEL. The L3E10 T cell hybridoma (anti-HEL108-116, I-E^d) was cocultured for 24 h with the A6B9 B cell lymphoma (H-2^d, FcγRIIb2^+) and various concentrations of HEL alone or in the presence of 0.2 μM of different wt or mutant anti-HEL Fv-MalE hybrids, corresponding to the variable regions of the anti-HEL mAb D1.3 or different mutants described in Table I (V_L::V_H-MalE(D54A) and V_H::V_L-MalE(W92A) are not shown for clarity), plus a mixture of two anti-MalE mAbs, 94.1 and 56.5 (0.13 μM each). IL-2 released by L3E10 after 24 h of culture with A6B9 was assessed by the CTLL proliferation assay. The same experimental results are plotted in two ways. *A*, The L3E10 IL-2 release (kcpm) is plotted against the total HEL concentration present in the cultures. *B*, The L3E10 IL-2 release (kcpm) is normalized against the HEL concentration theoretically complexed to the different anti-HEL Fv-MalE hybrids ([C]). For this calculation, we resolved, for each point of the plot, the following equation: (K'_d = $[HEL]_{free}$ × $[Fv\text{-}MalE]_{free}$/[C]) where ($[HEL]_{free}$ = $[HEL]_{total}$ − [C]) and ($[Fv\text{-}MalE]_{free}$ = $[Fv\text{-}MalE]_{total}$ − [C]).

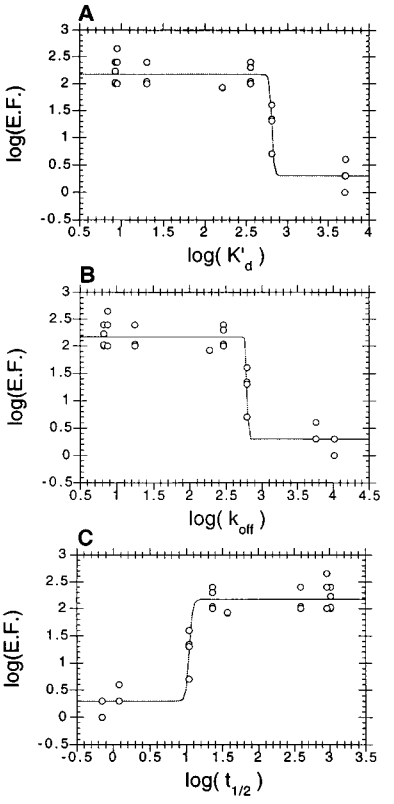

FIGURE 6. Relationship between the enhancement of HEL presentation and the binding parameters of the anti-HEL Fv-MalE. For each independent experiment in which the HEL presentation efficiency was compared in the presence or absence of the anti-HEL Fv-MalE and anti-MalE mAbs (as described in Fig. 5*A*), an EF was calculated as follow: EF = (HEL concentration required for 50% maximal IL-2 release by L3E10 in the absence of anti-HEL Fv-MalE)/(HEL concentration required for 50% maximal IL-2 release by L3E10 in the presence of anti-HEL Fv-MalE at 0.2 μM plus a mixture of the 2 anti-MalE mAbs 94.1 and 56.5 at 0.13 μM each). Each point represents an independent experiment. The same data are plotted in three different ways: log(EF) is plotted against log(K'_d) (nM) (*A*), log(k_{off}) (10^{-4} s^{-1}) (*B*), or log($t_{1/2}$) (s) (*C*) of the different anti-HEL Fv-MalE. The data shown in *A*, *B*, and *C* were fitted to the following equations (thin curves) using the Kaleidagraph software: Y = m1 + m2 × [1−1/(1 + exp(m3 × (m4 − X)))] in *A* and *B* and Y = m1 + m2/[1 + exp(m3 × (m4 − X))] in *C*. The correlation coefficients *r* obtained with these fittings were equal to 0.899 for the three plots. In these equations, (m1 + m2) and m1 define the maximal and minimal log(EF) values. m3 defines a cooperativity factor that is related to the sharpness of the transition between (m1) and (m1 + m2). m4 defines the X value for half transition. If X = m4, then Y = (m1 + m2/2). The values of the m1, m2, m3, and m4 parameters are given in Table II.

anti-MalE mAbs as shown above. The K_d values of the interaction between mAbs 94.1 and 56.5 and MalE are, respectively, equal to 7×10^{-10} M and 8×10^{-10} M. Thus, assuming two independent equilibriums in solution between Fv-MalE and each anti-MalE mAb, we calculated that, under the experimental conditions used, 100% of the Fv-MalE molecules were complexed by at least one anti-MalE mAb and that 42% were simultaneously complexed by the two anti-MalE mAbs. Thus, our experimental system was appropriate for evaluating the role of the affinity between Fv-MalE and HEL on the presentation of HEL since the capture of the different Fv-MalE hybrids by the FcγR-bearing APC was identical for all the hybrids tested. We then examined whether the efficiency of presentation to the T cells depended only on the concentration of bound HEL or also on the specific mutation of Fv-MalE. To address this question, the results of Figure 5*A* were plotted vs the amount of HEL theoretically complexed to the different Fv-MalE hybrids, assuming an equilibrium in solution. This representation showed clearly that, for the same concentration of complexed HEL, the Fv-MalE mutants did not increase HEL presentation to the T cell hybridoma with the same efficiency (Fig. 5*B*). In particular, V_L::V_H-MalE(Y101F) and V_L::V_H-MalE(D100N) were significantly less efficient in stimulating HEL presentation than the other Fv-MalE hybrids tested.

To clarify the relationship between affinity and HEL presentation, we analyzed the enhancement effect of the six Fv-MalE mutant hybrids. We calculated an EF equal to the ratio between the HEL concentrations required for half-optimal stimulation of the T cell hybridoma in the absence and in the presence of the complex between Fv-MalE and the anti-MalE mAbs. All the mutants shown in Table I were tested in at least two independent experiments. Figure 6 represents a synthesis of the results obtained with the

Table II. *Parameters obtained by fitting the variation of the enhancement of HEL presentation (enhancement factor) plotted against various binding parameters of the anti-HEL Fv-MalE (K'_d, k_{off}, or $t_{1/2}$)*

Type of Plot and Fitting	Parameters of the Fitting[a]			
	Maximal EF = $10^{(m1+m2)}$	Minimal EF = $10^{(m1)}$	Cooperativity factor = m3	Half transition value = $10^{(m4)}$
EF = f(K'_d)[b]	148-fold	Twofold	75	643 nM
EF = f(k_{off})[c]	148-fold	Twofold	137	622 10^{-4} s^{-1}
EF = f($t_{1/2}$)[d]	148-fold	Twofold	45	11 s

[a] The equations and the m1 to m4 parameters used for these fittings are described in Figure 6 legend.
[b,c,d] Plots and fittings shown in Figure 6, *A*, *B*, and *C*, respectively.

different Fv-MalE hybrids. Each point represents the enhancing effect of one Fv-MalE hybrid on HEL presentation obtained in an independent experiment. The EFs observed for the different anti-HEL Fv-MalE hybrids were plotted against their respective dissociation constant K'_d (nM) or k_{off} (10^{-4} s^{-1}) or $t_{1/2}$ (s) measured with the BIAcore apparatus (Fig. 6, *A*, *B*, and *C*, respectively). The EFs corresponding to the lowest values of K'_d (between 8.6 and 357 nM) were comparable and induced a 150- to 200-fold increase of HEL presentation. The EF rapidly decreased with affinity for intermediate values of K'_d. For the highest values of K'_d (around 5000 nM), the presentation of HEL was almost not affected by Fv-MalE. A similar relation between the EF and k_{off} was observed. This similarity is due to the fact that the increase in K'_d is mainly due to an increase of k_{off} (see Table I). The half-life ($t_{1/2}$) of the different complexes is inversely proportional to k_{off} and was consequently inversely related to the EF.

The enhancement effect on HEL presentation was at least twofold and was 148-fold at saturation (Table II). For the three plots, the transition between the virtual absence of enhancement effect and the plateau value was highly cooperative. The half transition values were K'_d = 643 nM, k_{off} = 622 10^{-4} s^{-1} and $t_{1/2}$ = 11 s. These values corresponded precisely to the binding parameters of V_L::V_H-MalE(Y101F) (Table I).

Discussion

The binding characteristics of Fv-MalE and HEL determine the efficiency of HEL presentation

In the present study, we analyzed the role of Ab affinity on Ab-mediated Ag uptake and presentation by APC using a new experimental system. In this system, the Ag (i.e., HEL) was captured by an anti-HEL Fv-MalE hybrid, which, in turn, was captured by anti-MalE mAbs via the FcγRIIb2 cellular receptor (Fig. 1). The subsequent FcγRIIb2-mediated endocytosis of these complexes resulted in the presentation of HEL by MHC II molecules. Indeed, the complexes formed between the T cell epitope (HEL 108–116) and the I-E^d molecule are recognized by the specific T cell hybridoma L3E10.

The stimulation of the T cells was measured as a function of the concentration of HEL present in the culture, using fixed concentrations of anti-HEL Fv-MalE hybrids and anti-MalE mAbs. For these reasons, we could consider that the internalization of the Fv-MalE by the anti-MalE mAbs was constant and independent of HEL capture. We calculated an EF to compare the efficiencies of HEL presentation by the FcγRIIb2-mediated endocytosis of the anti-MalE/Fv-MalE/HEL complex (arrow b in Fig. 1) and by the pinocytosis of HEL in fluid phase (arrow a in Fig. 1). We used Fv-MalE mutants with different affinities for HEL to analyze the relationship between their binding parameters and the EF. The results showed that only Fv-MalE hybrids having a sufficient affinity for HEL corresponding to a K'_d below a transition value equal to 643 nM enhanced the presentation of HEL with a maximal efficiency. In this range of K'_d, the maximum EF was approximately 148-fold. We found similar thresholds for k_{off} and $t_{1/2}$ due to the weak changes in k_{on} between the different hybrids tested. The saturation of the EF at the lowest K'_d values likely stemmed from a limitation of the Fv-MalE uptake by the A6B9 APC. Indeed, we observed, in the same antigenic system (HEL and L3E10 hybridoma) and with the same APC, EFs rising up to 1000-fold when HEL was captured by a mixture of two anti-HEL mAbs of high affinity (P. Guermonprez et al., manuscript in preparation). This last result rules out the possibility that the saturation of the EF observed here comes from a limitation of the sensitivity of the T cell assay that we used.

The K'_d and k_{off} of the Fv-MalE hybrids could affect the presentation at several levels. K'_d determines the efficiency of HEL complexation with Fv-MalE in the culture medium and, thus, the amount of HEL that is internalized. However, we found that, for a given amount of bound HEL, some hybrids triggered HEL presentation with lower efficiencies. This finding suggested strongly that the mutations influenced not only the level of HEL complexation but also later steps of its uptake and intracellular processing by the APC. Therefore, the binding characteristics of Fv-MalE and HEL could interfere either with the endocytosis or with the intracellular targeting and delivery of HEL.

Binding characteristics of Fv-MalE and HEL endocytosis

The half-life of the interaction between the Fv-MalE/anti-MalE complex and FcγR at the surface of the APC could constrain the rate of dissociation between Fv-MalE and HEL. The internalization of the Fv-MalE/anti-MalE complex by the APC occurred at a constant rate since Fv-MalE and the anti-MalE mAbs were at fixed concentrations in the presentation experiments. Therefore, HEL was internalized efficiently only if it did not dissociate before the internalization of the Fv-MalE/anti-MalE immune complexes via anti-MalE mAbs/FcγR interactions. Thus, the rate of HEL/Fv-MalE dissociation should be compared with the rate of the clearance of immune complexes (Fv-MalE/anti-MalE mAbs) from the membrane by the FcγR-mediated endocytosis. If the $t_{1/2}$ of the HEL/Fv-MalE complex is inferior to the $t_{1/2}$ of the Fv-MalE/anti-MalE mAbs complex at the surface of the cell (before endocytosis by FcγRIIb2), some of the Fv-MalE/anti-MalE mAbs complexes would not participate in HEL uptake, and, therefore, some HEL molecules that have been complexed with Fv-MalE/anti-MalE mAbs and fixed to FcγRIIb2 would not be internalized. Mellman et al. (16) have found that the $t_{1/2}$ of polyvalent immune complexes bound to the FcγR of macrophages is approximately 105 s. The half transition values of $t_{1/2}$ that we found here for the HEL/Fv-MalE complex is 11 s. The comparison of these two values strongly suggests that the half-life of the complexes between the Fv-MalE hybrids and HEL could be a factor limiting the internalization of HEL by the constitutive endocytosis of the Fv-MalE hybrids. This parameter could also influence the BCR-mediated internalization of Ag by specific B cells. Indeed, Watts and Davidson (17) have determined that the half-life of membrane Ig in human EBV-B cell lines is 8 min (480 s). This half-life would correspond to a limiting k_{off} of 14 × 10^{-4} s^{-1}. If the hypothesis developed above for the internalization of Fv-MalE through anti-MalE mAbs and FcγRIIb2 can be extrapolated to the internalization through BCR, then it would impose a rather high affinity for the BCR-mediated internalization of monovalent and soluble Ag by specific B cells for presentation to T cells at the beginning of a T cell-dependent humoral response.

Binding characteristics of Fv-MalE and intracellular targeting or delivery of HEL

The fate of internalized HEL could differ between the different Fv-MalE mutants, and this could influence the efficiency of HEL presentation. There still exists a controversy on the exact compartment where Ag processing takes place, and the physico-chemical environment where HEL is processed is not precisely known (3). Nevertheless, the mutations in the Fv regions of the hybrids could differentially affect the dynamics of intracellular HEL release. Indeed, Aluvihare et al. (18) showed that the quality of the Ag/BCR interaction could impose different degrees of dependence on the rapid intracellular delivery to the MHC II-processing compartment. In our case, this kind of limitation could explain why, at the same level of bound HEL, all Fv-MalE mutants did not trigger HEL presentation with the same efficiency. For Fv-MalE with the higher k_{off} (the shorter $t_{1/2}$), HEL could dissociate from Fv-MalE before reaching the right compartment for Ag processing. The mutations could also affect differentially the pH stability of the HEL/Fv-MalE interaction in the acid and reducing environment of the endocytic pathway and, thus, affect the efficiency of HEL processing (19).

Concluding remarks

The K'_d value that was required for the half optimal EF on HEL presentation (6.43×10^{-7} M) determined in this study corresponds approximately to the intermediate range of affinities that can be observed during the humoral immune response (6). This value cannot be extended to the internalization of Ag by the BCR due to possible differences between the behaviors of this receptor and of the immune complexes formed between Fv-MalE and anti-MalE mAbs. Thus, it should be relevant to test the impact of the mutations we studied here on the BCR (formed with the D1.3 Ig)-mediated presentation of HEL to T cells. Nevertheless, our results support the idea that affinity maturation may influence the Ag presentation to T cells by specific B cells. The hypothetical constraint on Ab k_{off} (or $t_{1/2}$) for Ag internalization due to the rate of receptor internalization (or half-life on cell surface of BCR) could be decreased for a polyvalent Ag such as hapten-carrier conjugates, as compared with a monovalent one such as HEL for two reasons. First, the avidity of an Ag for the BCR is increased by its polyvalence and, second, the receptor aggregation could accelerate the internalization of the complexes (20). These constraints on k_{off}, if physiologically relevant, could influence the affinity of B cell clones that are recruited in the preimmune repertoire by a T cell-dependent Ag. The fact that HEL Abs reach a high affinity in primary response (7) is especially relevant for the choice of this antigenic model. One can ask whether this fact relies on a bias on the naive B cell repertoire toward this Ag or whether it depends on a selective process that favors the expansion of high affinity B cell clones. Our results support the second hypothesis: weak affinity B cell clones might not be selected due to their inability to present the monomeric HEL to specific anti-HEL T helper cells to receive help for Ab production. Thus, priming of high affinity B cells in primary response could be a more general feature of strictly monovalent Ags (which is not the case of the well-described hapten-carrier systems as discussed above). The identification of this kind of constraint, even in an unphysiologic experimental system like the one we used, thus appears particularly relevant for the understanding of the dynamic of the Ab response.

References

1. Rock, K. L., B. Benacerraf, and A. K. Abbas. 1984. Antigen presentation by hapten-specific B-lymphocytes. I. Role of surface immunoglobulin receptors. *J. Exp. Med. 160:1102.*
2. Lanzavecchia, A. 1985. Antigen-specific interaction between T and B cells. *Nature 314:537.*
3. Watts, C. 1997. Capture and processing of exogenous antigens for presentation on MHC molecules. *Annu. Rev. Immunol. 15:821.*
4. Parker, D. C. 1993. T cell-dependent B cell activation. *Annu. Rev. Immunol. 11:331.*
5. Manca, F., D. Fenoglio, A. Li Pira, A. Kunkl, and F. Celada. 1991. Effect of antigen/antibody ratio on macrophage uptake, processing and presentation to T cells of antigen complexed with polyclonal antibodies. *J. Exp. Med. 137:37.*
6. Foote, J., and H. N. Eisen. 1995. Kinetic and affinity limits on antibodies produced during immune responses. *Proc. Natl. Acad. Sci. USA 92:1254.*
7. Newman, M. A., C. R. Mainhart, C. P. Mallett, T. B. Lavoie, and S.J. Smith-Gill. 1992. Patterns of antibody specificity during the BALB/c immune response to hen egg white lysozyme. *J. Immunol. 149:3260.*
8. Brégégère, F., J. Schwartz, and H. Bedouelle. 1994. Bifunctional hybrids between the variable domains of an immunoglobulin and the maltose-binding protein of *Escherichia coli*: production, purification and antigen binding. *Protein Eng. 7:271.*
9. England, P., F. Brégégère, and H. Bedouelle. 1997. Energetic and kinetic contributions of contact residues of antibody D1.3 in the interaction with lysozyme. *Biochemistry 36:164.*
10. Amit, A. G., R. A. Mariuzza, S. E. V. Phillips, and R. J. Poljak. 1986. Three-dimensional structure of an antigen-antibody complex at 2.8 Å resolution. *Science 233:747.*
11. Kim, K., C. Kanellopoulos-Langevin, R. M. Merwin, D. H. Sachs, and R. Asofsky. 1979. Establishment and characterization of BALB/c lymphoma lines with B cell properties. *J. Immunol. 122:549.*
12. Jones, B., J. P. Tite, and C. A. Janeway, Jr. 1986. Different phenotypic variants of the mouse B cell tumor A20/2J are selected by antigen- and mitogen-triggered cytotoxicity of L3T4-positive, I-A-restricted T cell clones. *J. Immunol. 136:348.*
13. Amigorena, S., C. Bonnerot, J. R. Drake, D. Choquet, W. Hunziker, J. G. Guillet, P. Webster, C. Sautes, I. Mellman, and W. H. Fridman. 1992. Cytoplasmic domain heterogeneity and functions of IgG Fc receptors in B lymphocytes. *Science 256:1808.*
14. Gengoux, C., and C. Leclerc. 1995. In vivo induction of $CD4^+$ T cell responses by antigens covalently linked to synthetic microspheres does not require adjuvant. *Int. Immunol. 7:45.*
15. Unkeless, J.C. 1979. Characterization of a monoclonal antibody directed against mouse macrophage and lymphocyte Fc receptors. *J. Exp. Med. 150:580.*
16. Mellman, I., and H. Plutner. 1984. Internalization and degradation of macrophage Fc receptors bound to polyvalent immune complexes. *J. Cell. Biol. 98:1170.*
17. Watts, C., and H. W. Davidson. 1988. Endocytosis and recycling of specific antigen by human B cell lines. *EMBO J. 7:1937.*
18. Aluvihare, V. R., A. A. Khamlichi, G. T. Williams, L. Adorini, and M. S. Neuberger. 1997. Acceleration of intracellular targeting of antigen by the B-cell antigen receptor: importance depends on the nature of the antigen-antibody interaction. *EMBO J. 12:3553.*
19. Jensen, P. E. 1995. Antigen unfolding and disulfide reduction in antigen presenting cells. *Sem. Immunol. 150:347.*
20. Song, W., H. Cho, P. Cheng, and S. K. Pierce. 1995. Entry of B cell antigen receptor and antigen into class II peptide loading compartment is independent of receptor cross-linking. *J. Immunol. 155:4255.*